Jornadas de Automática

Automated Image Analysis of CNS Cell Cultures Exposed to Microplastics

Rolhaiser-Pérez, Carina Viviana[a], Villarroya-Piqué, Gerard[b], Serrano-Pertierra, Esther[c,f], Fernandez-Sanchez, M. Teresa[c,f,g], Novelli, Antonello[d,f,g], McCarty, Alexander[c], Rio-Alvarez, Angel[e,g], Gonzalez, Víctor M.[b,g,*]

[a]*Nursery Faculty, University of Oviedo, Spain*
[b]*Electrical Engineering Department, University of Oviedo, Spain*
[c]*Biochemistry and Molecular Biology Department, University of Oviedo, Spain*
[d]*Psychology Department, University of Oviedo, Spain*
[e]*Computer Science Department, University of Oviedo, Spain*
[f]*University Institute of Biotechnology of Asturias (IUBA), University of Oviedo, Spain*
[g]*Biomedical Engineering Center (BME), University of Oviedo, Spain*

To cite this article: Rolhaiser-Pérez, Carina Viviana, Villarroya-Piqué, Gerard, Serrano-Pertierra, Esther, Fernandez-Sanchez, M. Teresa, Novelli, Antonello, McCarty, Alexander, Rio-Alvarez, Angel, González, Víctor M., 2025. Automated Image Analysis of CNS Cell Cultures Exposed to Microplastics. Jornadas de Automática, 46. https://doi.org/10.17979/ja-cea.2025.46.12164

Resumen

Este estudio evalúa los efectos de micro- y nanoplásticos de tereftalato de polietileno (PET) y polipropileno (PP) sobre cultivos primarios de células del sistema nervioso central (SNC), compuestos por neuronas y células gliales. Las células fueron expuestas durante 28 días a concentraciones de 100 y 500 µg/mL de PET y PP. Las imágenes obtenidas mediante microscopía de contraste de fases se analizaron con FIJI para cuantificar áreas vacías y la proliferación glial. Los resultados mostraron que PET100 y PP500 provocaron las alteraciones morfológicas más significativas, con aumento de zonas sin células y de células gliales, lo que sugiere una respuesta de estrés celular asociada a reactividad glial. La metodología aplicada permitió un seguimiento no invasivo a lo largo del tiempo, sin afectar la viabilidad celular. Estos hallazgos subrayan el potencial impacto neurotóxico de los microplásticos y respaldan el uso del análisis automatizado de imágenes como herramienta útil para evaluar contaminantes ambientales en modelos in vitro del SNC.

Palabras clave: Microplásticos, Nanoplásticos, Cultivos de Neuronas, Procesamiento de Imagen, Deep Learning.

Abstract

This study investigates the effects of polyethylene terephthalate (PET) and polypropylene (PP) micro- and nanoplastics on primary central nervous system (CNS) cell cultures containing neurons and glial cells. Cultures were continuously exposed for 28 days to PET and PP at 100 and 500 µg/mL. Phase-contrast microscopy images were acquired at multiple time points and analyzed using FIJI software to quantify non-cellular (void) areas and glial cell coverage. The most significant morphological alterations were observed in PET100 and PP500 conditions, showing increased void areas and glial proliferation compared to controls. These changes suggest a stress response consistent with glial reactivity. The method enabled non-invasive, longitudinal analysis without affecting cell viability and demonstrated the value of phase-contrast imaging for toxicological assessment. The approach proved reproducible and scalable, supporting its use in mechanistic studies. Overall, the findings highlight the potential neurotoxic impact of environmental microplastics and the usefulness of image-based tools for evaluating long-term effects in in vitro CNS models.

Keywords: Micro-plastics, Nano-plastics, CNS Cell Cultures, Deep Learning, Image Processing.

*Corresponding author: vmsuarez@uniovi.es

1. Introducción

Plastic pollution has become a global health and environmental concern due to the massive production and poor management of synthetic polymers. Among the most persistent and biologically active by-products of plastic degradation are microplastics (particles <5 mm) and nanoplastics (particles <1 μm), which result from the fragmentation of larger plastic items or are manufactured intentionally for use in industrial and consumer products (Shruti et al., 2023). These particles are widespread in aquatic environments, food chains, and even indoor air, increasing human exposure risk through ingestion, inhalation, and dermal contact.

Recent studies have confirmed the accumulation of micro- and nanoplastics in human tissues, including the gastrointestinal tract (Li et al., 2024), placenta (Ragusa et al., 2021), and even the brain (Nihart et al., 2025). Alarmingly, nanoplastics have also been detected in maternal breast milk (Bugatti et al., 2023), indicating potential early-life exposure. In patients with asymptomatic high-grade carotid artery stenosis, micro- and nanoplastics have been identified within atheromatous plaques, suggesting their role in inflammatory and thrombotic processes in vascular tissues.

Beyond their accumulation in critical organs, microplastics may affect systemic health through disruption of the intestinal microbiota. Studies suggest that ingested nanoplastics can alter the diversity and composition of the gut microbial ecosystem, favoring the growth of pro-inflammatory bacterial populations while reducing beneficial commensals (Li et al., 2024). This dysbiosis can contribute to chronic low-grade inflammation, immune system imbalance, and even neuroinflammation via the gut–brain axis. Given the established connection between gut health and neurological conditions, these findings highlight a potential indirect pathway by which environmental microplastics may influence CNS function.

At the cellular level, nanoplastics have been shown to induce inflammation, oxidative stress, and functional disruptions in neural systems. Microglial cells can internalize polystyrene nanoplastics, triggering reactive gliosis and altered gene expression linked to chronic neuroinflammation (Paing et al., 2024). Astrocytes, while not undergoing apoptosis, respond with increased reactivity (astrogliosis), a hallmark of neurotoxic stress (Jung and Ryu, 2025). These effects are especially concerning in the context of developing or aging brains, where cellular plasticity and resilience are compromised.

Despite these findings, many studies rely on endpoint observations using fixed or stained samples, which prevent continuous monitoring of culture dynamics and may introduce artifacts. There is a growing need for non-invasive methodologies capable of assessing the biological effects of environmental contaminants over time, especially in delicate cell systems such as primary cultures of CNS neurons and glial cells.

The main objective of this study has been to develop a non-invasive and automated methodology to assess the morphological impact of micro- and nanoplastics on CNS cell cultures. We propose the use of FIJI software (Schindelin et al., 2012) to quantify the proportion of void areas within the cultures and to quantify the number and distribution of glial cells in culture over time. By applying automated image processing techniques to phase contrast microscopy images, this work aims to provide a robust and reproducible tool for the evaluation of environmental neurotoxicants preserving culture viability and enabling longitudinal analysis.

The remainder of this paper is structured as follows: Section 2 describes the experimental design and the image processing techniques used. Section 3 presents the results of the image analysis. Section 4 discusses the implications of these findings, and Section 5 outlines the conclusions and future research directions.

2. Methods

2.1. Cell Culture Preparation

Primary cultures of central nervous system (CNS) cells were obtained from the cerebellum of Wistar rats aged 7–8 days. All procedures were conducted in compliance with ethical standards and approved protocols at the University of Oviedo. Cerebellar tissues were enzymatically dissociated and seeded into culture dishes, allowing for the coculture of neurons and glial cells.

From the first day of culture, cells were exposed to microplastic particles of two types: polyethylene terephthalate (PET) and polypropylene (PP), each at two concentrations: 100 μg/mL and 500 μg/mL. A control group was maintained under identical conditions without microplastic exposure. Cultures were incubated at 37 °C in a humidified atmosphere containing 5 % CO_2. To monitor morphological changes over time, phase-contrast images were acquired at four time points: days 5, 14, 18, and 28. For each condition and time point, six non-overlapping fields of view were captured using an Olympus IMT-2 inverted microscope equipped with a 10X objective. The resulting dataset provided a robust basis for image-based quantification of cell behavior across treatment conditions.

2.2. Image Acquisition and Processing

Images were captured in grayscale and stored in TIFF format at a resolution of 640x480 pixels (307,200 total pixels per image). All image processing was conducted using FIJI (ImageJ) (Schindelin et al., 2012), a distribution of ImageJ optimized for biological image analysis. Custom macros were developed to automate repetitive processing steps and standardize parameter application across all samples.

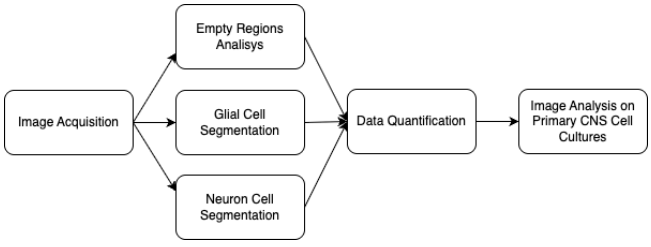

Figura 1: Schematic overview of the experimental design and image processing workflow.

Figure 1 summarizes the experimental and computational workflow from culture preparation to quantitative image analysis. After image acquisition three different processes are

applied in parallel in order to extract information that characterize the cultures behavior when subject to environments with microplastics: void areas quantification, glial cells and neurons.

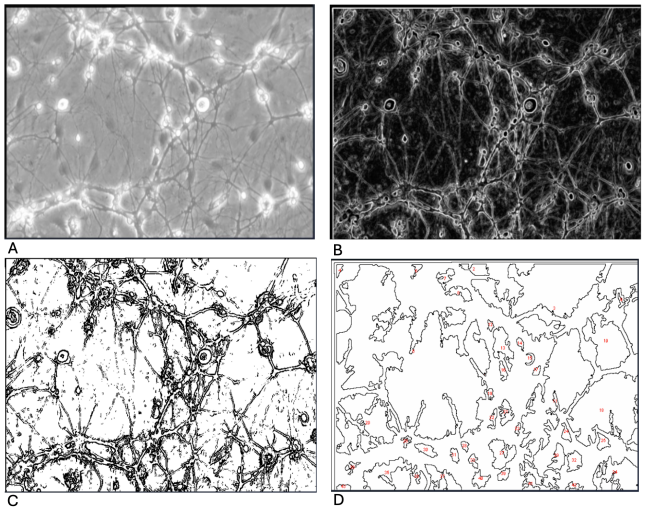

Figura 2: Neuron cultures images at several processing stages with FIJI to visualize void areas. A) Original image; B) After Find Edges filter; C) After Despeckle filter; D) Void areas identified after Analyze Particles filter.

2.3. *Quantification of Void Areas*

To assess cellular degradation or decreased confluence due to microplastic exposure, we quantified empty (non-cellular) regions in each image by applying the following filters (see Figure 2 for an example):

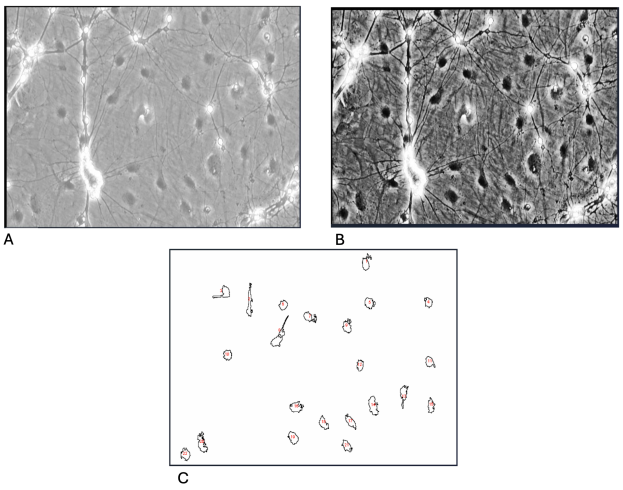

Figura 3: Culture images at several processing stages with FIJI to visualize glia cells. A) Original image. B) After Enhance Contrast filter. C) Glia cells identified after Analyze Particles filter.

- First, the `Find Edges` filter was applied to enhance cellular boundaries.
- The resulting image was binarized using automatic thresholding, followed by the `Despeckle` function to remove noise, i.e., small artifacts, while strengthening the big artifacts.
- Using `Analyze Particles` filter, objects were filtered by size (minimum 150 px) and circularity (0.00–1.00). Particles smaller than 10,000 px were excluded to avoid counting small intercellular gaps or artifacts.
- The void area was calculated as the cumulative area of the remaining objects, expressed as a percentage of the total image area (307,200 px).

The process was fully automated using a FIJI macro and the output exported in CSV format for statistical analysis.

2.4. *Glial Cells Analysis*

To evaluate the response of glial cells, mainly astrocytes, to exposure to the plastics, the following procedure was applied:

- Image contrast was enhanced using the `Enhance Contrast` tool with the option `Histogram Equalization` enabled.
- A manual threshold was adjusted per image to distinguish astrocytes from background based on typical morphology and intensity. `Dark Background` option should be disabled to assure that the astrocytes highlight white over black.
- `Analyze Particles` was then run with a size threshold of 150 px and circularity range 0.10–1.00.
- The background was set to light and objects were counted based on area and shape descriptors.
- Output metrics included total cell count, individual and mean cell area, perimeter, and circularity.

Figure 3 shows an example of this procedure. As with the void area analysis, custom macros ensured reproducibility across datasets. The data were compiled and analyzed using Microsoft Excel and FIJI's Results Table export.

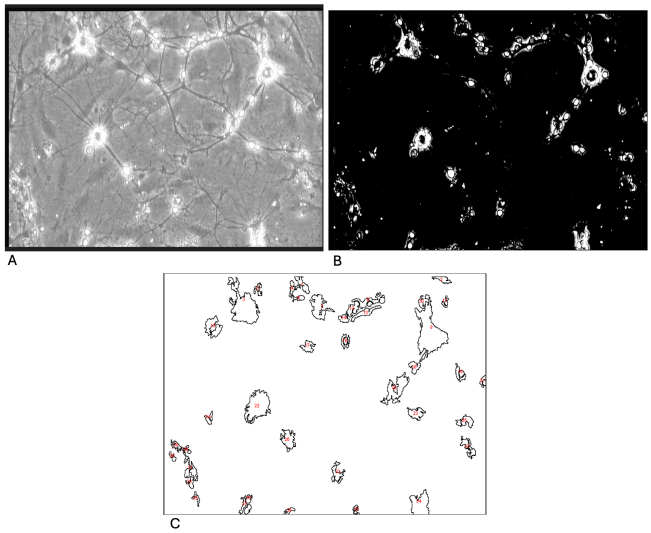

Figura 4: Culture images at several processing stages with FIJI to visualize neuron cells. A) Original image; B) After Brightness Threshold filter; C) Neuron cells identified after Analyze Particles filter.

2.5. *Neurons Analysis*

In order to analyze the behavior of neurons due to exposure to the microplastics, the following processing procedure was applied (see Figure 4 for an example):

- A brightness threshold was applied to binarized the image using the `Brightness & Contrast` tool.
- The most adequate threshold for each image was calculated manually. It was found that for these data set images, 200 was an optimum value for most cases.
- `Analyze Particles` was then run with a size threshold of 100 px and circularity range 0.10–1.00.
- Output metrics included total cell count, individual and mean cell area, perimeter, and circularity.

2.6. *Reproducibility and Data Handling*

All image processing steps were standardized using macros and documented parameter sets. Intermediate outputs were visually inspected to confirm segmentation accuracy. CSV files were structured to facilitate downstream statistical analysis, and all scripts are available upon request.

3. Results

Exposure to PP and PET resulted in an increased percentage of empty areas in the cultures. The area and number of glial cells showed condition-dependent variations, with PET100 and PP500 showing an increase in the number of glial cells at intermediate and late stages of exposure. These changes were observed consistently across multiple images, validating the robustness of the automated approach. Results for neuronal counting were less consistent across experiments: in some cases the total number of neurons in culture was not affected over time, while in other experiments a decrease in the number of neurons in culture was observed. More experiments are needed to extract sound conclusions.

The remaining of this section presents the quantitative results obtained from image analysis of primary CNS cell cultures exposed to microplastics. Results are organized by measurement type: void area, glial cell area, and glial cell number, as can be seen in Table 1. No results for neuronal counting are presented until more experiments are conducted. Data were extracted from six non-overlapping microscopy images per condition at four time points: days 5, 14, 18, and 28.

3.1. *Void Area Analysis*

Figure 5 shows the evolution of the percentage of void (empty) area in the cell cultures. In the control group, a gradual increase in empty space was observed, reaching 27.10 % at day 28, likely due to natural culture aging. In contrast, microplastic-treated cultures exhibited a significantly higher void percentage.

PET100 showed an increase from 22.97 % (day 5) to 63.86 % (day 28), while **PP500** peaked at 52.13 % (day 14), dropped to 40.84 % (day 18), and then reached 73.43 % at day 28. On the other hand, **PET500** and **PP100** showed moderate increases with smoother fluctuations.

These results suggest that exposure to PET100 and PP500 may have affected the cellular adhesion mechanisms of glial and neuronal cells to the culture dish surface, causing the observed increase in the non-cellular surface over time.

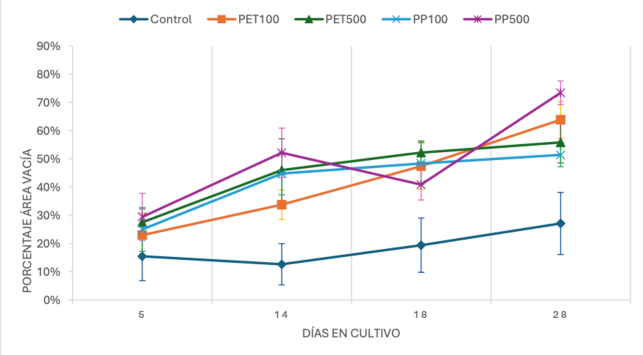

Figura 5: Void area percentage evolution between days 5 and 28 for different treatment conditions.

3.2. *Glial Cell Area Occupation*

Figure 6 illustrates the relative area occupied by glial cells. The control condition showed steady growth from day 5 to day 28, reaching 3.89 %. Treatments with PET and PP produced distinct patterns.

While **PET100** peaked at 4.50 % on day 18, and then slightly decreased to 3.85 %, **PET500** remained stable around 4 % before falling to 3.35 %. On the other hand, **PP100** fluctuated more, with 4.44 % on day 5 and 3.26 % at the endpoint, and **PP500** showed progressive growth, reaching 4.32 % at day 14 and stabilizing near 4.12 %.

These results may be consistent with glial activation due to the presence of PET100 and PP500 in the culture medium

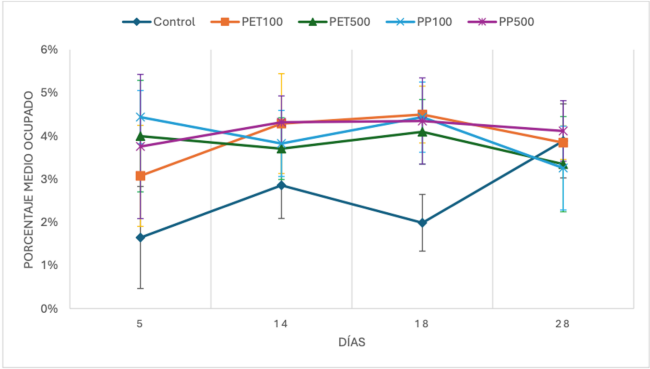

Figura 6: Area occupied by glial cells evolution between days 5 and 28 for different treatment conditions

3.3. *Total Glial Cell Count*

The total number of glial cells per image, see Figure 7, also varied across conditions. While the control culture increased from approximately 12 to 22 cells/image between day 5 and 28, **PET100** and **PET500** showed higher counts, reaching up to 50 cells/image. On the other hand, **PP100** fluctuated and declined slightly toward the final time point, and **PP500** increased steadily, with some variability, reaching values comparable to PET100.

These data support the hypothesis that exposure to PET and PP microplastics can cause alterations in morphology and division rate of CNS glial cells.

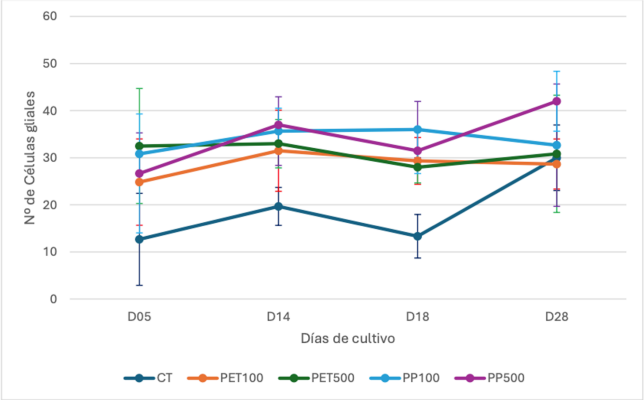

Figura 7: Average number of glial cells evolution between days 5 and 28 for different treatment conditions.

3.4. Interpretation of Cell Morphology and Viability

Although total cell count did not drastically differ across groups, qualitative differences in distribution, morphology, and organization were observed. Cultures treated with microplastics tended to show disrupted spatial arrangements and morphological abnormalities in the present glial cells. These may indicate functional changes not captured by density metrics alone, warranting further investigation via complementary imaging and molecular assays Li et al. (2024); Paing et al. (2024); Jung and Ryu (2025).

4. Discussion

The results presented in this study demonstrate that exposure to microplastics—specifically PET and PP at concentrations of 100 µg/mL and 500 µg/mL—induces measurable morphological changes in CNS cells in primary culture. Cultures treated with these particles exhibited higher void areas, increased glial cell coverage, and elevated glial cell counts compared to untreated controls. Among all tested conditions, PET100 and PP500 induced the most pronounced effects, indicating that effects of these toxicants may depend on polymer type and concentration.

The changes in morphology we observed align with growing evidence showing that micro- and nanoplastics accumulate in human tissues. Particles have been found in the gastrointestinal tract, placenta, and even the brain Li et al. (2024); Ragusa et al. (2021); Nihart et al. (2025). Brain accumulation, in particular, raises concerns about long-term neurotoxic effects, especially in vulnerable populations. Although our model is in vitro, the observed disruption of culture integrity and glial overactivation suggest that microplastics may have direct structural and functional consequences on CNS cells under prolonged exposure.

Previous studies have shown that polystyrene nanoplastics can lead to the activation of microglia, trigger neuroinflammation, and alter gene expression in exposed neural tissues Paing et al. (2024). These effects could be responsible for the effects we observed in this study. Likewise, astrocytes are known to undergo reactive astrogliosis under neurotoxic stress without direct apoptosis Jung and Ryu (2025), consistent with our morphological observations.

Furthermore, indirect systemic mechanisms such as gut–brain axis signaling have been proposed as potential pathways for microplastic-induced neurotoxicity. Ingested microplastics can disrupt the gut microbiota, leading to dysbiosis and the release of pro-inflammatory signals that affect the brain Li et al. (2024). Although this mechanism was not directly assessed here, our findings complement such hypotheses by revealing cellular changes consistent with chronic inflammatory stress.

This study demonstrates the utility of automated image analysis for non-invasive monitoring of culture viability. By segmenting void areas and glial cells from phase-contrast images using FIJI Schindelin et al. (2012), we obtained robust indicators of culture health without the need for cell staining. This enables longitudinal studies and enhances reproducibility.

However, there are limitations to acknowledge. Phase-contrast imaging lacks molecular specificity, and threshold-based segmentation may introduce operator bias despite standardization. The classification of glial cells was based on morphological features and should be validated using immunofluorescence markers in future work. The dataset could also benefit from dynamic analysis or time-lapse imaging to understand the temporal evolution of microplastic effects more accurately.

In summary, this study reinforces existing concerns about the neurobiological impact of microplastics. Even in the absence of direct toxicity to neurons, structural degradation and glial activation suggest significant stress responses in CNS cultures. These findings warrant further investigation using more complex co-culture models, molecular profiling, and integration with gut microbiota-derived signals to better understand the systemic risks posed by environmental plastic exposure.

5. Conclusions

This study provides experimental evidence that exposure to micro- and nanoplastics, specifically PET and PP particles, induces significant morphological changes in primary central nervous system (CNS) cell cultures. Using a non-invasive image analysis pipeline, we demonstrated that treated cultures exhibit increased void areas and enhanced glial cell proliferation compared to untreated controls. These effects were especially pronounced for PET100 and PP500 conditions, regardless of dose.

Our findings are consistent with recent reports of microplastic accumulation in human tissues and their potential to trigger neuroinflammatory responses through direct cellular contact or systemic pathways. Although this work was conducted in a simplified in vitro system, the structural disruptions and glial responses observed reflect key aspects of environmental neurotoxicity.

The methodological approach employed, based on phase-contrast imaging and automated segmentation, proved effective in quantifying culture integrity and glial behavior over time

without compromising cell viability. This supports the use of label-free image analysis as a valuable tool for environmental toxicology research.

FIJI-based image processing provides an effective and scalable method for analyzing morphological changes in CNS cultures exposed to microplastics. The findings emphasize the importance of automated, non-invasive tools for neurotoxicological research and reinforce the need for further studies into environmental pollutants' neurological impact.

Future studies should incorporate molecular assays, neuronal markers, and dynamic imaging techniques to explore mechanisms of toxicity more comprehensively. Integrating microbiota–brain axis models may also help elucidate indirect pathways of plastic particle effects on the CNS.

In conclusion, our results underscore the need for further investigation into the biological impacts of environmental plastic contamination and advocate for increased attention to microplastic exposure as a factor in neurological health.

Acknowledgments

This research has been funded by the Spanish Ministry of Economics and Industry –grant PID2020-112726RB-I00–, the Spanish Research Agency –grant PID2023-146257OB-I00–, and Missions Science and Innovation project MIG-20211008 (INMERBOT). Also, by Principado de Asturias, grants SV-PA-21-AYUD/2021/50994 and AYUD/2023/36906/UO-077, and by the Council of Gijón through the University Institute of Industrial Technology of Asturias grants SV-21-GIJON-1-19, SV-22-GIJON-1-19, SV-22-GIJON-1-22, SV-23-GIJON-1-17, and SV-24-GIJON-1-18. Finally, this research has also been funded by Fundación Universidad de Oviedo grants FUO-23-008 and FUO-22-450.

CRediT authorship contribution statement

Carina Viviana Rolhaiser-Pérez: Writing – original draft, Software, Investigation. **Gerard Villarroya-Piqué:** Writing – review and editing, Writing – original draft, Visualization, Validation, Investigation, Data curation. **Esther Serrano-Pertierra:** Writing – review and editing, Writing – original draft, Visualization, Validation, Methodology, Investigation, Formal analysis, Data curation, Conceptualization. **M. Teresa Fernandez-Sanchez:** Writing – review and editing, Writing – original draft, Visualization, Validation, Methodology, Investigation, Formal analysis, Data curation, Conceptualization, Resources. **Antonello Novelli:** Writing – review and editing, Writing – original draft, Visualization, Validation, Methodology, Investigation, Formal analysis, Data curation, Conceptualization, Resources. **Alexander McCarty:** Visualization, Data curation. **Angel Rio-Alvarez:** Writing – review and editing, Writing – original draft, Visualization, Validation, Methodology, Investigation, Formal analysis, Data curation, Conceptualization, Project administration, Supervision. **Víctor M. González:** Writing – review and editing, Writing – original draft, Visualization, Validation, Methodology, Investigation, Formal analysis, Data curation, Conceptualization, Project Administration, Resources, Funding acquisition.

Ethics statement

All procedures in this research were conducted in compliance with applicable laws and institutional guidelines. The research did not require ethical approval as it was not conducted on human subjects or animals. The authors confirm that no ethical complications were identified during the course of the study.

Declaration of competing interest

The authors declare that they have no known competing financial interests or personal relationships that could have appeared to influence the work reported in this paper.

Declaration of generative AI in scientific writing

ChatGPT and Grammarly were used in the writing process to improve the readability and language of the manuscript.

Referencias

Bugatti, C., Almeida, K. d., Guimarães, M. d. A., Amâncio, N. d. F., 2023. Microplásticos e nanoplásticos e sua relevância na saúde humana: uma revisão de literatura. Research, Society and Development 12 (1). DOI: 10.33448/rsd-v12i1.38949

Jung, B., Ryu, K., 2025. Lipocalin-2: a therapeutic target to overcome neurodegenerative diseases by regulating reactive astrogliosis. Experimental & Molecular Medicine. DOI: 10.1038/s12276-023-01098-7

Li, W., Zhang, X., Liu, J., Wang, Y., Guo, X., 2024. Microplastic-induced gut microbiota dysbiosis: a review of the mechanisms and health implications. Frontiers in Cellular and Infection Microbiology 14, 1492759. DOI: 10.3389/fcimb.2024.1492759

Nihart, A., Garcia, M., El Hayek, E., Liu, R., Olewine, M., Kingston, J., et al., 2025. Bioaccumulation of microplastics in decedent human brains. Nature Medicine 31 (2), 215–220. DOI: 10.1038/s41591-024-03453-1

Paing, Y., Eom, Y., Song, G., et al., 2024. Neurotoxic effects of polystyrene nanoplastics on memory and microglial activation: Insights from in vivo and in vitro studies. Science of The Total Environment 924. DOI: 10.1016/j.scitotenv.2024.171681

Ragusa, A., Svelato, A., Santacroce, C., Catalano, P., Notarstefano, V., Carnevali, O., et al., 2021. Plasticenta: First evidence of microplastics in human placenta. Environment International 146, 106274. DOI: 10.1016/j.envint.2020.106274

Schindelin, J., Arganda-Carreras, I., Frise, E., Kaynig, V., Longair, M., Pietzsch, T., et al., 2012. Fiji: an open-source platform for biological-image analysis. Nature Methods 9 (7), 676–682. DOI: 10.1038/nmeth.2019

Shruti, V., Kutralam-Muniasamy, G., Pérez-Guevara, F., 2023. Do microbial decomposers find micro- and nanoplastics to be harmful stressors in the aquatic environment? a systematic review of in vitro toxicological research. Science of The Total Environment 903. DOI: 10.1016/j.scitotenv.2023.166561

	VOID AREA				GLIAL CELLS COUNT				GLIAL CLs' OCCUPIED AREA			
ID	**DAY 05**	**DAY 14**	**DAY 18**	**DAY 28**	**D05**	**D14**	**D18**	**D28**	**D05**	**D14**	**D18**	**D28**
CT_1	3.99 %	20.4 %	9.59 %	36.51 %	9	16	9	36	1.22 %	1.49 %	1.37 %	3.90 %
CT_2	15.32 %	5.3 %	35.75 %	17.72 %	1	22	10	34	0.12 %	3.48 %	1.32 %	4.39 %
CT_3	19.9 %	8.2 %	18.4 %	37.9 %	24	20	22	38	2.1 %	2.6 %	3.2 %	5.5 %
CT_4	4.3 %	22.1 %	15.1 %	13.3 %	11	26	12	21	1.5 %	3.9 %	2.1 %	3.3 %
CT_5	25.2 %	16.3 %	9.5 %	39.6 %	6	19	14	24	1.0 %	2.9 %	2.3 %	3.3 %
CT_6	24.1 %	3.5 %	28.0 %	17.6 %	25	15	13	27	3.9 %	2.7 %	1.6 %	3.0 %
MEAN	**15.5 %**	**12.6 %**	**19.4 %**	**27.1 %**	**13**	**20**	**13**	**30**	**1.7 %**	**2.9 %**	**2.0 %**	**3.9 %**
SD	**9.45**	**8.00**	**10.53**	**12.07**	**10**	**4**	**5**	**7**	**1.30**	**0.84**	**0.72**	**0.94**
PET100_1	12.4 %	24.4 %	51.5 %	68.1 %	9	39	38	36	0.9 %	5.1 %	5.1 %	4.2 %
PET100_2	24.2 %	33.5 %	34.8 %	68.8 %	37	28	26	23	4.6 %	4.1 %	3.6 %	3.8 %
PET100_3	28.8 %	30.8 %	56.9 %	57.4 %	26	25	32	31	3.8 %	3.4 %	4.9 %	3.5 %
PET100_4	26.1 %	35.6 %	39.9 %	52.7 %	25	45	26	31	2.9 %	6.4 %	4.3 %	4.0 %
PET100_5	33.2 %	37.3 %	56.3 %	65.7 %	29	29	29	22	3.7 %	3.7 %	5.3 %	3.3 %
PET100_6	13.0 %	40.9 %	45.1 %	70.4 %	23	23	25	29	2.6 %	3.1 %	3.7 %	4.4 %
MEAN	**23.0 %**	**33.7 %**	**47.4 %**	**63.9 %**	**25**	**32**	**29**	**29**	**3.1 %**	**4.3 %**	**4.5 %**	**3.9 %**
SD	**8.48**	**5.71**	**9.03**	**7.14**	**9**	**9**	**5**	**5**	**1.28**	**1.27**	**0.72**	**0.43**
PET500_1	28.3 %	45.1 %	46.6 %	68.4 %	36	36	27	40	4.6 %	4.4 %	4.1 %	3.4 %
PET500_2	28.8 %	24.5 %	50.4 %	51.2 %	39	35	29	23	4.7 %	3.9 %	3.8 %	3.3 %
PET500_3	18.0 %	44.3 %	52.4 %	53.3 %	35	23	32	50	4.3 %	2.4 %	4.3 %	5.2 %
PET500_4	29.3 %	47.0 %	57.3 %	55.6 %	32	32	29	28	3.3 %	3.3 %	4.8 %	3.0 %
PET500_5	27.1 %	56.9 %	57.7 %	60.9 %	9	36	29	29	1.5 %	3.8 %	4.9 %	3.7 %
PET500_6	33.7 %	58.4 %	49.0 %	45.6 %	44	36	22	15	5.6 %	4.5 %	2.7 %	1.5 %
MEAN	**27.5 %**	**46.0 %**	**52.2 %**	**55.8 %**	**32**	**33**	**28**	**31**	**4.0 %**	**3.7 %**	**4.1 %**	**3.3 %**
SD	**5.18**	**12.15**	**4.49**	**7.95**	**12**	**5**	**3**	**12**	**1.41**	**0.78**	**0.82**	**1.21**
PP100_1	32.2 %	39.9 %	47.0 %	56.7 %	24	28	34	32	3.2 %	2.8 %	4.8 %	2.7 %
PP100_2	25.8 %	48.4 %	51.1 %	56.2 %	35	35	35	24	4.8 %	4.6 %	4.6 %	2.8 %
PP100_3	33.0 %	42.7 %	49.3 %	49.0 %	31	40	33	47	4.9 %	4.9 %	3.7 %	4.8 %
PP100_4	27.6 %	59.1 %	62.1 %	50.7 %	36	27	42	19	4.7 %	3.2 %	5.0 %	1.9 %
PP100_5	21.3 %	43.6 %	38.6 %	44.3 %	28	46	28	50	4.9 %	4.1 %	3.1 %	4.3 %
PP100_6	9.9 %	35.1 %	42.1 %	51.6 %	31	38	44	24	4.2 %	3.4 %	5.4 %	3.0 %
MEAN	**25.0 %**	**44.8 %**	**48.4 %**	**51.4 %**	**31**	**36**	**36**	**33**	**4.4 %**	**3.8 %**	**4.4 %**	**3.3 %**
SD	**8.53**	**8.26**	**8.16**	**4.63**	**4**	**7**	**6**	**13**	**0.68**	**0.84**	**0.89**	**1.06**
PP500_1	16.8 %	52.5 %	45.9 %	72.6 %	32	37	36	46	4.2 %	4.5 %	5.2 %	4.6 %
PP500_2	31.8 %	67.5 %	50.2 %	68.6 %	27	38	33	41	3.9 %	5.0 %	5.3 %	3.9 %
PP500_3	31.5 %	41.4 %	35.8 %	73.0 %	28	43	23	47	3.8 %	5.1 %	2.8 %	3.8 %
PP500_4	33.5 %	43.3 %	36.6 %	76.3 %	34	37	30	30	4.9 %	4.3 %	3.7 %	2.9 %
PP500_5	20.8 %	50.6 %	40.3 %	69.2 %	2	34	31	42	0.3 %	3.6 %	3.7 %	4.6 %
PP500_6	42.1 %	57.5 %	36.2 %	80.8 %	37	33	36	46	5.6 %	3.5 %	5.5 %	5.0 %
MEAN	**29.4 %**	**52.1 %**	**40.8 %**	**73.4 %**	**27**	**37**	**32**	**42**	**3.8 %**	**4.3 %**	**4.4 %**	**4.1 %**
SD	**9.15**	**9.60**	**5.97**	**4.58**	**13**	**4**	**5**	**6**	**1.83**	**0.67**	**1.09**	**0.77**

Tabla 1: Observed data for control cultures (CT_X) and experimental cultures subject to different microplastics at day 5, day 14, day 18 and day 28 organized into three types of measurements: void area, number of glial cells found, and area occupied by glial cells.